

Comparing reactions of H and Cl with C–H stretch-excited CHD₃

Jon P. Camden, Hans A. Bechtel, Davida J. Ankeny Brown, and Richard N. Zare^{a)}
Department of Chemistry, Stanford University, Stanford, California 94305-5080

(Received 6 September 2005; accepted 22 November 2005; published online 20 January 2006)

We report the methyl radical product state distributions for the reactions of H and Cl with CHD₃($\nu_1=1,2$) at collision energies of 1.53 and 0.18 eV, respectively. Both reactions demonstrate mode selectivity. The resulting state distributions from the H+CHD₃($\nu_1=1,2$) reactions are well described by a spectator model. The reactions Cl+CHD₃($\nu_1=1,2$) exhibit similar behavior, but in some aspects the spectator model breaks down. We attribute this breakdown to enhanced intramolecular vibrational redistribution in the Cl+CHD₃($\nu_1=1,2$) reactions compared to the H+CHD₃($\nu_1=1,2$) reactions, caused by the interaction of the slower Cl atom with the vibrationally excited CHD₃, which is promoted either by its longer collision duration, its stronger coupling, or both. © 2006 American Institute of Physics. [DOI: 10.1063/1.2155434]

I. INTRODUCTION

The outcome of a chemical reaction can be controlled, in certain circumstances, by using a laser to excite specific molecular vibrations.^{1–3} In a series of experiments Crim and co-workers^{4–10} and Zare and co-workers^{11–13} demonstrated the preferential cleavage (bond selectivity) of the O–H or O–D bond in the reactions of HOD with H, O, and Cl atoms by exciting either the O–H or O–D stretch, respectively. Crim and co-workers also observed mode-specific behavior in the reactions of H with H₂O prepared in the nearly isoenergetic $|04\rangle^-$ or $|13\rangle^-$ states, where $|ab\rangle$ is a shorthand for the number of quanta (a and b) in each O–H bond. Excitation of the $|04\rangle^-$ state produced mainly OH($\nu=0$) whereas excitation of the $|13\rangle^-$ state produced mainly OH($\nu=1$). A simple spectator model, in which the vibrational energy in the unreactive bond does not participate in the reaction, was proposed to account for the observed bond-selective and mode-selective behaviors. This spectator model was also found to be qualitatively correct for the reactions of chlorine with vibrationally excited methane.^{14–21}

Trajectory calculations of Schatz *et al.*²² were qualitatively able to reproduce the bond-selective behavior and demonstrated that the reaction H+HOD($\nu_{\text{O–D}}=7$)→H₂+OD is enhanced by several orders of magnitude over that of the ground state, even though the excitation is localized in the unreactive bond. These results suggest a breakdown of the spectator model: vibrational motion localized in the OD oscillator is able to enhance the reactivity of H-atom abstraction in the H+HOD reaction. The failure of the spectator model is intimately connected with intramolecular vibrational redistribution²³ (IVR), i.e., the way energy flows between the different internal modes of a molecule. Even if a vibrational eigenstate can be prepared in the reactant valley, the initially prepared vibrational motion might be partitioned into other modes as the system progresses over the barrier and onto the product valley. The details of this energy flow

are determined by the amount of time available for the interaction of the incoming atom with the excited reagent and the coupling between the modes of the reactive complex. This description assumes, of course, that motion on only one potential-energy surface suffices to describe the reaction dynamics, i.e., nonadiabatic behavior is assumed to be negligible.

Our laboratory in collaboration with Schatz and co-workers has recently performed an extensive study of the H+CD₄($\nu=0$) reaction.^{24–26} In that work we examined the CD₃ product state and angular distributions as a function of collision energy, comparing them to predictions from various full-dimensional potential-energy surfaces. We have also measured the vibrational enhancement factor and CH₃ state distributions for the H+CH₄(ν_3) reaction.²⁷ Attention is drawn to a recent review by Murray and Orr-Ewing²⁸ for a compilation of work on the Cl+CH₄ reaction before 2004. Since that time, however, several new studies have been completed by Liu and co-workers,^{29–31} Crim and co-workers,³² Orr-Ewing and co-workers,³³ and Zare and co-workers.^{18,34,35}

In this work we investigate the CD₃/CHD₂ product state distributions from the H+CHD₃($\nu_1=1,2$) and Cl+CHD₃($\nu_1=1,2$) reactions, where ν_1 is the C–H stretching vibration. We observe that the H-atom reactions are closer to the pure spectator limit, whereas the Cl-atom reactions are more bond selective. Our results illustrate that the identity of the attacking atom can dramatically influence the bond and mode selectivities observed for the same initially prepared methane vibration. The observed differences suggest a redistribution of the initially prepared vibration during the course of the reactive encounter.

A. Infrared spectroscopy of CHD₃($\nu_1=1$)

Normal modes are usually used to describe the vibrational motions in a polyatomic molecule.³⁶ Because the normal modes of a molecule constitute a complete basis set, any arbitrary motion can be described by the linear superposition of these modes. The CHD₃ molecule belongs to the C_{3v} point

^{a)}Author to whom correspondence should be addressed. Electronic mail: zare@stanford.edu

TABLE I. Normal-mode frequencies in cm^{-1} of CHD_3 , CHD_2 (Ref. 61) and CD_3 (Ref. 61).

CHD_3	CHD_2	CD_3
2993 (ν_1) C–H symmetric stretch	3114 (ν_1) C–H stretch	2158 (ν_1) symmetric stretching
2142 (ν_2) C–D symmetric stretch	2187 (ν_2) C–D asymmetric stretch	458 (ν_2) umbrella bending
1003 (ν_3) umbrella	1006 (ν_3) scissors	2381 (ν_3) antisymmetric stretching
2263 (ν_4) C–D antisymmetric stretch	431 (ν_4) out of plane	1026 (ν_4) deformation
1291 (ν_5) rock	2358 (ν_5) C–D asymmetric stretch	
1036 (ν_6) deformation	1248 (ν_6) C–H bend	

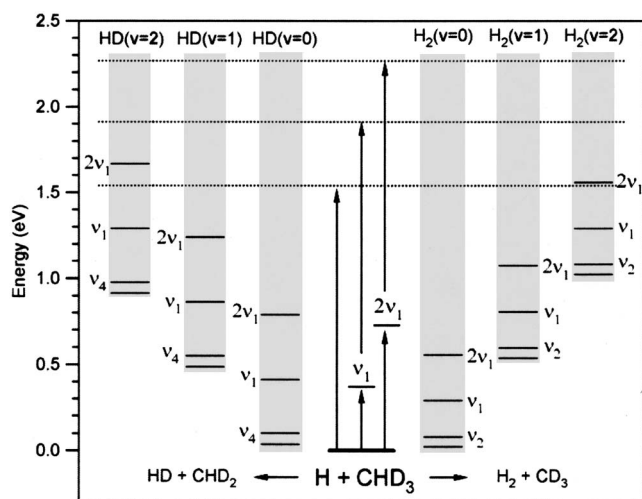
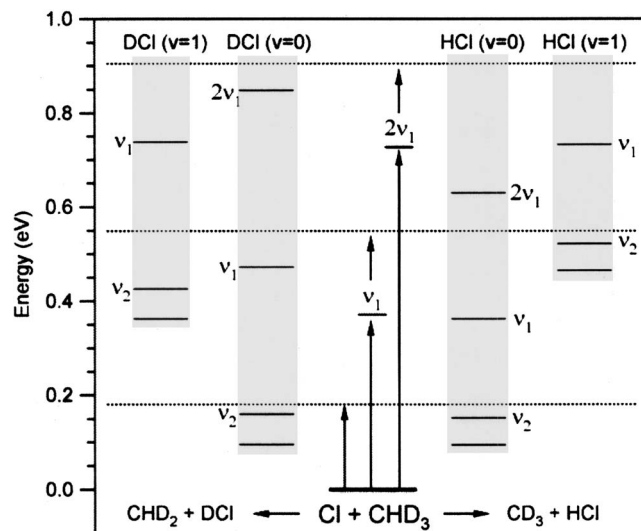
group and has six normal modes of vibration, which are listed in Table I. Upon isotopic substitution of CH_4 , the totally symmetric ν_1 mode transforms to the totally symmetric ν_1 mode in CHD_3 and becomes infrared active. The $2\nu_1(A_1)$ mode of CHD_3 is also accessible by one-photon IR absorption. For electric-dipole-allowed transitions between nondegenerate levels in molecules of C_{3v} symmetry, the $\Delta K=0$ selection rule leads to a parallel band, i.e., the transition dipole moment lies along the symmetry axis, and the molecular transition displays simple P , Q , and R branches. The K sublevels are beyond the resolution of the IR laser used in this experiment.

Some normal modes are isolated in a particular bond or region of a molecule; e.g., the ν_1 mode of CHD_3 corresponds mainly to stretching of the C–H bond due to the large mass difference between the H and D atoms. More generally, the X–H stretching vibrations and their overtones have proven to be particularly good examples of localized vibrations. A desire to model this behavior and the recognition that one is not restricted to using the normal-mode basis set has led theorists to develop the local-mode description of vibrational modes, in which each bond is treated as an independent anharmonic oscillator.^{37–43} In general, localization of the vibration occurs when the interbond coupling is weak and the bond anharmonicity is large. The infrared spectroscopy of the C–H chromophore has been the subject of detailed investigations^{44–47} and is known to be well described by the local-mode picture.⁴⁸ In particular, the $\text{CHD}_3(\nu_1=1,2)$ vibration is localized in the C–H oscillator and in the local-mode basis set we denote $\text{CHD}_3(\nu_1=1)$ as $|1000\rangle$, whereas $\text{CHD}_3(\nu_1=2)$ is

given by $|2000\rangle$. Our previous work has illustrated that the local-mode basis set is particularly useful in understanding the reactions of stretch-excited methane with both Cl (Refs. 15 and 49) and H.²⁷

B. Reaction energetics

The $\text{H}+\text{CH}_4\rightarrow\text{CH}_3+\text{H}_2$ reaction is nearly thermoneutral [$\Delta H(0\text{ K})=-9\times 10^{-4}\text{ eV}$] (Ref. 50) and has a large classical barrier to reaction [0.64 eV calculated at the CCSD(T) level with complete basis set extrapolation using CCSD(T)/cc-pVTZ geometries].²⁴ The $\text{Cl}+\text{CH}_4$ reaction, on the other hand, is slightly endoergic⁵¹ ($\Delta H=0.07\text{ eV}$) and has an estimated activation barrier⁵² of 0.34 eV. The vibrationally adiabatic ground-state barrier, which is a better predictor of threshold energies neglecting tunneling, of 0.17 eV.^{52,53} To calculate the energetics for the $\text{H}+\text{CHD}_3$ and $\text{Cl}+\text{CHD}_3$ reactions, we use the harmonic approximation, noting selected product state energies. The normal-mode frequencies of CD_3 and CHD_2 are given in Table I. The results of these calculations are shown in Fig. 1 for the $\text{H}+\text{CHD}_3$ reaction and in Fig. 2 for the $\text{Cl}+\text{CHD}_3$ reaction. We note that the H-atom and Cl-atom reactions have markedly different collision energies (E_{coll}), 1.52 and 0.18 eV, respectively, and therefore these two reactions have different energetically allowed product state channels. This situation arises because of the mass combinations of the photolytic precursors for the two reactions as well as the mass combinations of the two reactions.⁵⁴

FIG. 1. Energetics for the $\text{H}+\text{CHD}_3$ reaction.FIG. 2. Energetics for the $\text{Cl}+\text{CHD}_3$ reaction.

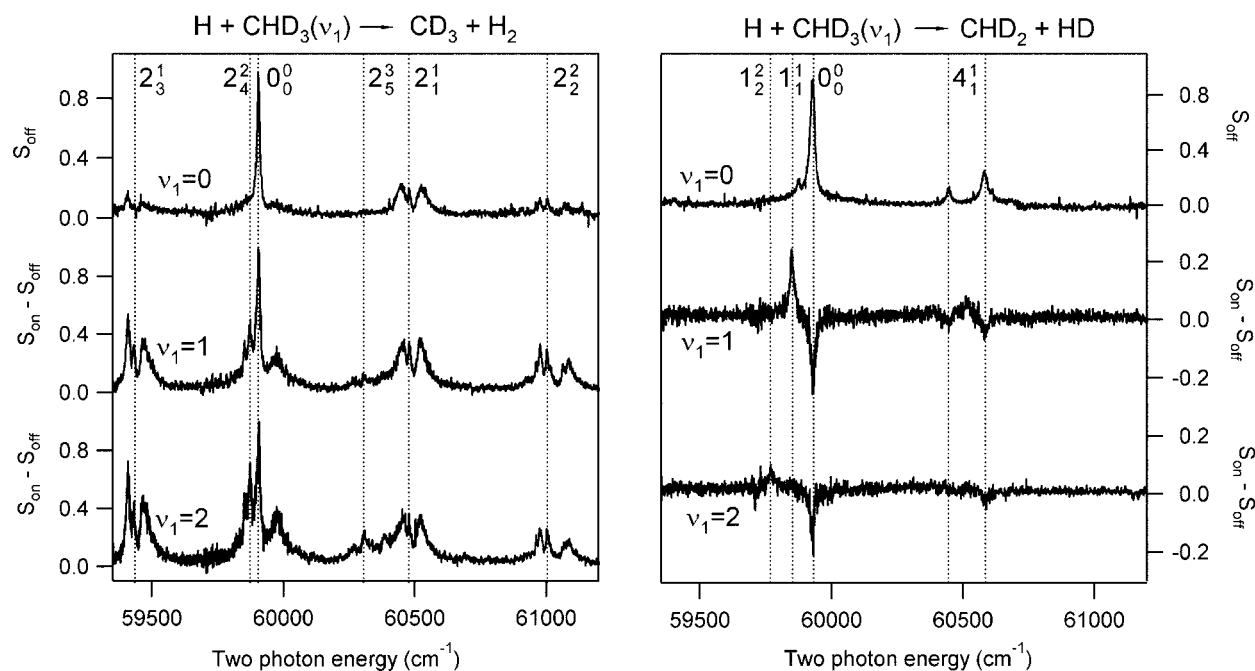


FIG. 3. REMPI spectra of the CD₃ (left panel) and CHD₂ (right panel) products from the H+CHD₃($\nu_1=0$) (top traces), H+CHD₃($\nu_1=1$) (middle traces), and H+CHD₃($\nu_1=2$) (bottom traces) reactions at a collision energy of 1.53 eV. The CD₃ and CHD₂ spectra are recorded simultaneously for each reaction.

II. EXPERIMENT

The experimental apparatus has been described in detail elsewhere,⁵⁵ therefore, only the most salient features are described here. Hydrogen bromide (Matheson, 99.999%) or molecular chlorine (Matheson, 99.999%), methane-d₃ (Cambridge Isotope Laboratories, 98%), and helium (Liquid Carbonic, 99.995%) are mixed in a glass bulb and delivered to a pulsed supersonic nozzle (General Valve, Series 9, 0.6 mm orifice, backing pressure \sim 700 torr). The resulting molecular beam enters the extraction region of a Wiley-McLaren time-of-flight spectrometer where it is intersected by three laser beams that prepare the reagent quantum state, initiate the reaction, and state-selectively probe the products.

The CHD₃ symmetric stretching fundamental or overtone is prepared by direct infrared absorption around 3.3 or 1.7 μ m respectively. Fast H atoms are generated by the 230 nm photolysis of HBr,⁵⁶ and fast Cl atoms are generated from the 355 nm photolysis of Cl₂.⁵⁷ The photolysis of Cl₂ at 355 nm produces monoenergetic Cl atoms in their ground electronic state. The photolysis of HBr at 230 nm produces mainly fast H atoms, i.e., those coincident with ground-state Br; however, a small fraction (\sim 15%) comes with spin-orbit excited Br* and is referred to as the slow channel. This channel might be a cause for some concern; however, we have made a study of the collision energy dependence of both the vibrational enhancement and the methyl radical state distribution for the related H+CH₄($\nu_3=1,2$) \rightarrow CH₃+H₂ reaction, and we found no change over the 1.5–2.2 eV energy range.²⁷ Therefore, we feel that the small contribution of the slow channel to these current experiments does not significantly affect our conclusions. After a time delay of 20–30 ns for the H-atom reaction and 70–100 ns for the Cl-atom reaction, the nascent CD₃ and CHD₂ reaction products are state-selectively ionized using a 2+1 resonance-enhanced multi-

photon ionization (REMPI) scheme via the $3p_z^2A_2'' \leftarrow X^2A_2''$ transition⁵⁸ for CD₃ and via the $3p^2B_1 \leftarrow X^2B_1$ transition⁵⁹ for CHD₂. In order to ensure that no bias exists in the measurements from faster moving products flying out of the probe volume before the slower moving ones, all measurements were made at a time delay for which the CD₃/CHD₂ product signal was still a linear function of the time delay. The product ions separate according to their mass and are detected by microchannel plates. In the current experiments, both the $m/z=17$ and 18 mass peaks were recorded simultaneously as a function of the REMPI laser wavelength. Large extraction fields (800 V/cm) are used while scanning the REMPI spectra in order to collect all ions of a given mass that are formed in the focal volume of the probing laser. To distinguish between the CD₃/CHD₂ products from the reaction of mainly ground-state methane in the molecular beam and the CD₃/CHD₂ products from the reaction with vibrationally excited methane, the IR light is modulated on and off on a shot-by-shot basis. Subtraction of the signals that result when the IR laser is on (S_{on}) and off (S_{off}) gives the difference signal ($S_{on}-S_{off}$), which is a measure of the enhancement from vibrational excitation of the CHD₃ reagent.

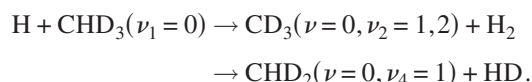
Excitation of CHD₃($\nu_1=1$) requires light around 3.3 μ m, whereas CHD₃($\nu_1=2$) requires light around 1.7 μ m. Tunable infrared light around 1.7 μ m is generated by mixing the visible output of a Nd³⁺: YAG (yttrium aluminum garnet) (Continuum PL9020) pumped dye laser (Continuum, ND6000; Exciton, DCM) with the 1.064 μ m YAG fundamental in a beta barium borate (BBO) crystal. The 1.7 μ m light is then parametrically amplified in a LiNbO₃ crystal which is pumped by 1.064 μ m radiation. Using this scheme, we obtained \sim 20 mJ after the difference frequency stage and \sim 55 mJ after amplification. The same scheme was used to obtain 3.3 μ m light; however, instead of using the

amplified 1.7 μm light from the LiNbO_3 optical parametric amplification stage, the 3.3 μm beam (~ 12 mJ) was used. The 230 nm light (3–5 mJ) was generated by frequency tripling in two BBO crystals the output of a Nd^{3+} : YAG- (Continuum PL8020) pumped dye laser (Spectra Physics, PDL3; Exciton, LDS 698). The ~ 330 nm REMPI probe light (1.5 mJ) was generated by frequency doubling in a BBO crystal the output of a Nd^{3+} : YAG- (Spectra Physics DCR-2A) pumped dye laser (Lambda Physik, FL2002; Exciton, DCM/LDS698 mixture).

III. RESULTS

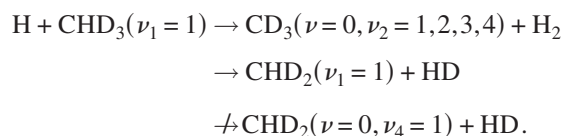
A. Reactions of H with $\text{CHD}_3(\nu_1=0, 1, 2)$

Figure 3 displays the REMPI spectra obtained for the CD_3/CHD_2 products from the reactions of H with $\text{CHD}_3(\nu_1=0, 1, 2)$ at $E_{\text{coll}}=1.53$ eV. The signal from the ground-state reaction, obtained when the IR laser is off, originates from the reactions with vibrationally unexcited CHD_3 . The difference signal, $S_{\text{on}}-S_{\text{off}}$, is shown for when the IR laser pumps the Q branch of the $\text{CHD}_3(\nu_1=1)$ and $\text{CHD}_3(\nu_1=2)$ transitions. The CD_3 and CHD_2 products are monitored simultaneously as the REMPI laser is scanned by detecting both the $m/z=17$ and 18 fragments. All spectra are obtained under similar experimental conditions; thus, although quantitative determinations of the state distribution are complicated owing to a modest signal-to-noise ratio and the effect of power broadening,⁶⁰ we believe that we can make some meaningful comparisons between the spectra. The ground-state reaction [Fig. 3(a)] shows no clear preference for the H- or D-abstraction products. We note, however, that isotopic substitution of the CD_3 to CHD_2 is expected to decrease the sensitivity of the CHD_2 REMPI transitions owing to the larger amount of predissociation⁵⁹ of the intermediate electronic state. Thus, the direct comparison of the exact branching ratio between H/D abstraction is difficult. The qualitative behavior, however, is clear especially in light of the spectra that result from the reactions of H/Cl with vibrationally excited CHD_3 , *vide infra*. Both reaction channels produce methyl fragments in their ground state or with low-frequency bending excitation, i.e., umbrella bending $\text{CD}_3(2_1^1)$ and out-of-plane large amplitude (OPLA) for $\text{CHD}_2(4_1^1)$. Small features are also observed that correspond to CD_3 fragments with several quanta of bending (2_2^2 and 2_3^1) and to CHD_2 fragments with C–D bending excitation (3_1^1). The major ground-state reaction channels can be summarized as

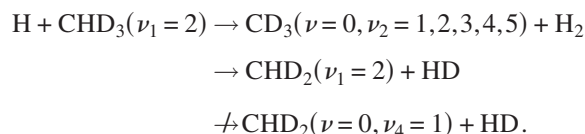


Upon vibrational excitation of the C–H stretching chromophore dramatic changes are observed. Several new features appear in the spectra of the CD_3 and CHD_2 product channels. Higher overtones of the CD_3 umbrella bending motion are observed as hot bands ($2_3^1, 2_4^2$, and 2_3^3) whose fraction increases from $\text{H}+\text{CHD}_3(\nu_1=1)$ to $\text{H}+\text{CHD}_3(\nu_1=2)$. Even more striking differences appear in the CHD_2 spectra. A large depletion is observed on the 0_0^0 and 4_1^1 bands;

therefore, the cross section for forming ground-state and OPLA CHD_2 products is smaller for the vibrationally excited CHD_3 molecules. We also observe the formation of C–H stretch-excited CHD_2 in the appearance of the 1_1^1 band. The major reaction channels for the fundamental excited reaction can be summarized as



This trend continues with excitation of the first C–H stretching overtone of CHD_3 . In the CHD_2 spectrum, the 0_0^0 depletion signal remains, the 1_1^1 band is no longer present, and a new band, which we attribute to 1_2^2 , appears. This assignment is made on the basis of the calculated vibrational frequencies of the ground and excited electronic states of CHD_2 and the known selection rules from Brum *et al.*⁵⁹ The depletion for the $\text{CHD}_3(\nu_1=2)$ spectrum is likely smaller because it is harder to saturate the IR pumping step. One important consideration in the above spectra is what fraction of the methane molecules is pumped to the excited state with the IR laser. From the observed depletion signal on the $\text{CHD}_2 0_0^0$ band we estimate the fraction $N[\text{CHD}_3(\nu_1=1)]/N[\text{CHD}_3(\nu=0)]$ to be greater than 0.2 and $N[\text{CHD}_3(\nu_1=2)]/N[\text{CHD}_3(\nu=0)]$ to be greater than 0.1, where N is the number of molecules. We note that this estimate does not rely on any assumptions about the spectator model but rather is derived simply from the ratio of the signals with the IR pump laser on and off. The major reaction channels for the overtone excited reaction are summarized as



B. Reactions of Cl with $\text{CHD}_3(\nu_1=0, 1, 2)$

State distributions and angular distributions for the HCl fragment have previously been reported by Simpson *et al.*¹⁴ for the $\text{Cl}+\text{CHD}_3(\nu_1=1)$ reaction and we do not focus on them in this work. Figure 4 displays the CD_3 and CHD_2 REMPI spectra obtained for the $\text{Cl}+\text{CHD}_3(\nu_1=0, 1, 2)$ reactions at $E_{\text{coll}}=0.18$ eV with similar conditions as Fig. 3. Several differences are noted immediately. The ground-state reaction, $\text{Cl}+\text{CHD}_3(\nu=0)$, produces methyl fragments in their ground vibrational state only, due to energetic constraints, and the ratio of the CD_3 products to the CHD_2 products is larger. The difficulties in determining the quantitative H/D abstraction ratio presented in Sec. III A do not affect this conclusion, as the REMPI spectra were obtained under similar experimental conditions. The fact that the energy available to the Cl-atom reaction is much closer to threshold suggests that the difference in zero-point energies of the C–H and C–D bonds could explain the larger CD_3/CHD_2 ratio in the Cl-atom reaction when compared to the H-atom reaction.

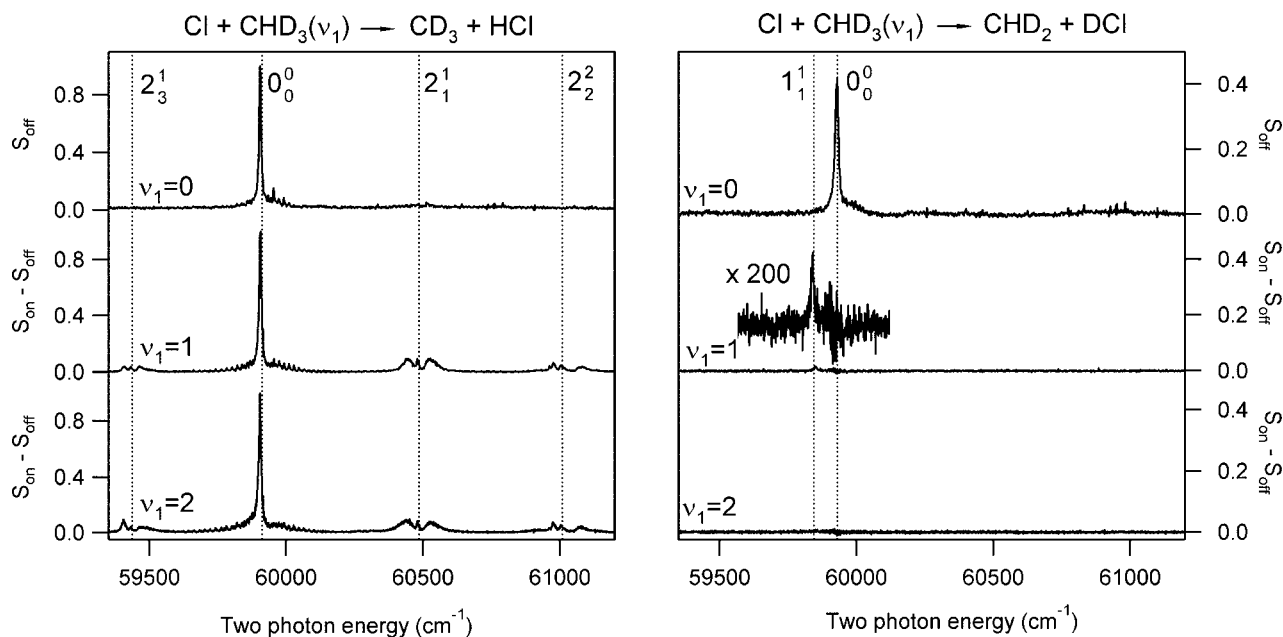
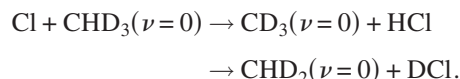
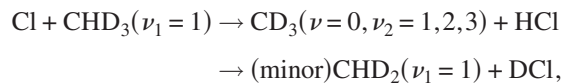


FIG. 4. REMPI spectra of the CD₃ (left panel) and CHD₂ (right panel) products from the Cl+CHD₃($\nu_1=0$) (top traces), Cl+CHD₃($\nu_1=1$) (middle traces), and Cl+CHD₃($\nu_1=2$) (bottom traces) reactions at a collision energy of 0.18 eV. The CD₃ and CHD₂ spectra are recorded simultaneously for each reaction.

The main reaction channels are



Upon C–H stretch excitation of CHD₃ the CD₃ products are formed primarily in their ground state, in contrast to the H-atom reaction. A small but increasing fraction of the CD₃ products is bend excited as the number of C–H stretching quanta of the methane reagent increases. The reaction of CHD₃($\nu_1=1$) with Cl exhibits a strong preference for the H-abstraction channel, but a very small amount of the channel leading to CHD₂($\nu_1=1$) is observed. Lastly, the reaction of Cl with CHD₃($\nu_1=2$) leads to similar behavior, except that no stretch-excited CHD₂ is observed, although this may simply be caused by a lack of sensitivity. Summarizing the reaction channels of Cl with CHD₃(ν_1),



The most striking differences between the H- and Cl-atom reactions occur upon C–H stretch excitation of CHD₃, as can be seen by comparing Figs. 3 and 4. The H-atom reaction with CHD₃(ν_1) leads to a depletion of the ground-state CHD₂ products, production of C–H stretch-excited CHD₂, and excitation of the CD₃ bending modes. The same initially prepared vibration for the Cl-atom reaction shows no depletion signal, an extremely small amount of C–H stretch-excited CHD₂, and less preference for CD₃ bending mode excitation.

IV. DISCUSSION

A. Spectator model

We begin by briefly reviewing the spectator model and giving a clear description of the assumptions we use in the following discussion. For a polyatomic molecule such as methane we define the pure spectator limit as one in which every bond acts as a local uncoupled oscillator. In this crude picture we neglect bending motions and assume that every C–H bond is independent of all others. Further, the initial vibration is given by the local-mode description.

The CHD₃($\nu_1=1,2$) vibration is localized in the C–H oscillator. In the local-mode basis set we denote CHD₃($\nu_1=1$) as $|1000\rangle$ and CHD₃($\nu_1=2$) as $|2000\rangle$. In this simple picture, the H/Cl atom has a choice when it approaches the vibrating methane. Reaction with the C–H oscillator will leave the CD₃ fragment in its ground vibrational state, whereas reaction with a C–D bond will leave CHD₂ fragments with one quantum of C–H stretching. Thus, there is no mechanism for the formation of ground-state CHD₂ products. This model applies equally to the reaction of $|2000\rangle$ excited CHD₃, except in this case reaction with a C–D oscillator will lead to CHD₂ products with two quanta of CH stretching. An interesting prediction of this model is that the reaction cross section for forming ground-state CHD₂ fragments should actually be smaller in the vibrationally excited reactions, a point that has not been addressed until this work. Of course, we might also ask if the initially localized excitation can facilitate cleavage of the unexcited C–D bonds, as was suggested by the trajectory calculations of Schatz *et al.*²² Table II displays the state-selected ratios of $\sigma_{\nu_1}/\sigma_{\text{gs}}$ that result from predictions of the isolated bond model. If the ratio is greater than ($>$), equal to ($=$), or less than ($<$) 1, the vibrationally excited cross section is larger, equal to, or smaller than the ground-state reaction, respectively. For sim-

TABLE II. Observed ratio of the vibrationally excited to ground-state reaction cross section. If the ratio is greater than ($>$), equal to ($=$), or less than ($<$) 1, the vibrationally excited cross section is larger, equal to, or smaller than the ground-state reaction, respectively. The expected value of this ratio obtained from the spectator model is given for comparison. It is not possible to put the experiment on an absolute scale, so that the prediction of 0 is in accord with the depletion of the product, which is indicated by $<$. The H-atom reactions are seen to be in good agreement with the model, whereas the Cl-atom reactions show some clear disagreements, which are indicated by the asterisk (*).

	CHD ₂ ($\nu=0$)		CHD ₂ ($\nu_1=1$)		CHD ₂ ($\nu_1=2$)		CD ₃ ($\nu=0$)	
	Model	Expt.	Model	Expt.	Model	Expt.	Model	Expt.
H+CHD ₃ 1000)	0	$<$	$>$	$>$	0	0	$>$	$>$
Cl+CHD ₃ 1000)	0*	$=$ *	$>$ *	~ 0 *	0	0	$>$	$>$
H+CHD ₃ 2000)	0	$<$	0	0	$>$	$>$	$>$	$>$
Cl+CHD ₃ 2000)	0*	$=$ *	0	0	$>$	0*	$>$ *	$>$

plicity, we exclude the umbrella bending products in this treatment. A zero indicates that the product state is not expected for a given reaction channel.

B. Comparing the H- and Cl-atom reactions

We first consider the reactions of H and Cl to form ground-state CHD₂. Recall that $S_{\text{off}} \propto \sigma_{\nu=0}$ and $S_{\text{on}} \propto (1-x)\sigma_{\nu=0} + x\sigma_{\text{IR}}$ and their ratio is given by

$$\frac{\sigma_{\text{IR}}}{\sigma_{\nu=0}} = \frac{(S_{\text{on}}/S_{\text{off}} - 1)}{x} + 1.$$

Therefore, if $S_{\text{on}}/S_{\text{off}}=1$, which results when $S_{\text{on}}-S_{\text{off}}=0$, then the ratio of the cross sections is also unity and the ground-state and vibrationally excited reactions have the same cross section. In practice, it is hard to determine whether a difference signal of zero arises because (1) the ratio of the cross sections is actually unity or (2) the small positive or negative signal is below the experimental sensitivity. However, this ambiguity is removed in the current experiments because of the clear depletion observed for the H+CHD₃($\nu_1=1,2$) \rightarrow CHD₂($\nu=0$)+HD reactions. The IR pumping scheme was not changed between the two reactions; therefore it is clear that the cross section for forming ground-state CHD₂ from the reactions Cl+CHD₃($\nu_1=1,2$) is comparable to that of the Cl+CHD₃($\nu=0$) reaction.

A positive, zero, or negative signal provides a direct measurement of the ratio of the ground-state and excited-state cross sections. These measurements are tabulated along with the values expected for the spectator model in Table II. Depletion of a product, denoted by $<$, is considered to be in rough agreement with the model prediction of 0. It is clear that the H-atom reaction is in better agreement with the model than the Cl-atom reaction, which shows marked disagreements in several cases. For example, the cross sections for formation of ground-state CHD₂ from the reaction of C–H stretch-excited and ground-state CHD₃ are approximately equal, contrary to the predictions of the spectator model. Therefore, when a D atom is abstracted from C–H stretch-excited CHD₃, the vibration must flow from the C–H bond into the translation of the escaping product fragments or the internal excitation of the DCl modes. In either case, the vibration does not remain localized during the reaction, which contradicts the spectator model. This behavior is also

observed for the reaction Cl+CHD₃($\nu_1=2$) in which the cross section for CHD₂($\nu=0$) is about the same as that for the reaction Cl+CHD₃($\nu=0$). In this case, the breakdown of the spectator model is even more accentuated as two quanta of C–H stretching must flow from the C–H bond, which leaves the CHD₂ product vibrationless.

It might be argued that in the normal-mode picture, the ν_1 vibration is not entirely localized in the C–H bond but has a small amount in the C–D bonds, which might explain the ability of the methane vibration to promote abstraction of the C–D bonds and leave the CHD₂ fragment in its ground state in the Cl-atom reaction, but we can rule out such a possibility because of our results for the H-atom reaction. If this were the case, then we might expect to see either (a) a similar enhancement in the H-atom reaction or (b) a small amount of CD₃ products formed with stretch excitation.

One curious feature that we observe is rather large excitation of the bending modes, up to five quanta in umbrella bending in CD₃, which occurs in the H-atom reactions when compared to the Cl-atom reaction. In all cases, the ratio of the umbrella bend-excited CD₃ products to the ground-state CD₃ is larger for the H-atom reactions, although we point out that the fraction of energy deposited into the bending mode is still small when compared to the total energy available. Our REMPI spectra suggest that the initially prepared vibration is more effectively transferred into the product bending modes in the H-atom reaction than the Cl-atom reaction. Neither the spectator picture nor a simple adiabatic picture of the dynamics is able to rationalize this behavior. Our experiments suggest that excitation of the stretching motion in CHD₃ leads nonadiabatically to ground-state methyl fragments in the Cl+CHD₃($\nu_1=1,2$) reactions, whereas stretching excitation leads nonadiabatically to bend-excited methyl fragments in H+CHD₃($\nu_1=1,2$).

The present study clearly indicates that intramolecular vibrational redistribution (IVR) takes place to various extents during the course of the reactions, more for Cl+CHD₃($\nu_1=1,2$) and much less for H+CHD₃($\nu_1=1,2$). In our previous study²⁷ of the reactions H/Cl+CH₄($\nu_3=1,2$) we proposed that the difference in interaction time could account for the major observed differences in the Cl- and H-atom reactions. While it is true that the H atom approaches more quickly than the Cl atom and thus leaves less time for the vibration to be localized into the reactive bond, we need to include the

possibility that the Cl atom may couple more strongly than the H atom in the course of the reaction. Both effects may be at work. The exact details are not possible to extract from the present study, and more experiments as well as more theoretical studies are needed to elucidate the nature of the IVR for this chemical reaction.

In summary, we have studied the CD₃/CHD₂ state distributions that result from the reactions of H and Cl with CHD₃($\nu_1=0,1,2$). Notable differences exist between the two reactions: particularly, the H-atom reaction appears to be in closer accord with the pure spectator model. A simple explanation based on the greater importance of IVR for Cl +CHD₃(ν_1) is proposed to account for the different behaviors found in these two related reaction systems. Although IVR seems to be more pronounced for the Cl-atom reaction with C–H stretch-excited CHD₃, the vibrational redistribution must contribute to the stronger bond selectivity of this reaction.

ACKNOWLEDGMENTS

Two of the authors (J.P.C. and H.A.B.) thank the National Science Foundation for graduate fellowships. This work was supported by National Science Foundation Grant No. 0242103.

- ¹F. F. Crim, *J. Phys. Chem.* **100**, 12725 (1996).
- ²F. F. Crim, *Acc. Chem. Res.* **32**, 877 (1999).
- ³R. N. Zare, *Science* **279**, 1875 (1998).
- ⁴A. Sinha, M. C. Hsiao, and F. F. Crim, *J. Chem. Phys.* **92**, 6333 (1990).
- ⁵A. Sinha, M. C. Hsiao, and F. F. Crim, *J. Chem. Phys.* **94**, 4928 (1991).
- ⁶A. Sinha, J. D. Thoemke, and F. F. Crim, *J. Chem. Phys.* **96**, 372 (1992).
- ⁷J. M. Pfeiffer, R. B. Metz, J. D. Thoemke, E. Woods, and F. F. Crim, *J. Chem. Phys.* **104**, 4490 (1996).
- ⁸J. M. Pfeiffer, E. Woods, R. B. Metz, and F. F. Crim, *J. Chem. Phys.* **113**, 7982 (2000).
- ⁹M. C. Hsiao, A. Sinha, and F. F. Crim, *J. Phys. Chem.* **95**, 8263 (1991).
- ¹⁰R. B. Metz, J. D. Thoemke, J. M. Pfeiffer, and F. F. Crim, *J. Chem. Phys.* **99**, 1744 (1993).
- ¹¹M. J. Bronikowski, W. R. Simpson, B. Girard, and R. N. Zare, *J. Chem. Phys.* **95**, 8647 (1991).
- ¹²M. J. Bronikowski, W. R. Simpson, and R. N. Zare, *J. Phys. Chem.* **97**, 2194 (1993).
- ¹³M. J. Bronikowski, W. R. Simpson, and R. N. Zare, *J. Phys. Chem.* **97**, 2204 (1993).
- ¹⁴W. R. Simpson, T. P. Rakitzis, S. A. Kandel, A. J. Orr-Ewing, and R. N. Zare, *J. Chem. Phys.* **103**, 7313 (1995).
- ¹⁵Z. H. Kim, H. A. Bechtel, and R. N. Zare, *J. Am. Chem. Soc.* **123**, 12714 (2001).
- ¹⁶H. A. Bechtel, Z. H. Kim, J. P. Camden, and R. N. Zare, *J. Chem. Phys.* **120**, 791 (2004).
- ¹⁷H. A. Bechtel, J. P. Camden, D. J. A. Brown, and R. N. Zare, *J. Chem. Phys.* **120**, 5096 (2004).
- ¹⁸Z. H. Kim, H. A. Bechtel, J. P. Camden, and R. N. Zare, *J. Chem. Phys.* **122**, 084303 (2005).
- ¹⁹S. Yoon, S. Henton, A. N. Zivkovic, and F. F. Crim, *J. Chem. Phys.* **116**, 10744 (2002).
- ²⁰S. Yoon, R. J. Holiday, and F. F. Crim, *J. Chem. Phys.* **119**, 4755 (2003).
- ²¹S. Yoon, R. J. Holiday, E. L. Sibert, and F. F. Crim, *J. Chem. Phys.* **119**, 9568 (2003).
- ²²G. C. Schatz, M. C. Colton, and J. L. Grant, *J. Phys. Chem.* **88**, 2971 (1984).
- ²³D. J. Nesbitt and R. W. Field, *J. Phys. Chem.* **100**, 12735 (1996).
- ²⁴J. P. Camden, H. A. Bechtel, D. J. A. Brown, M. R. Martin, R. N. Zare, W. Hu, G. Lendvay, D. Troya, and G. C. Schatz, *J. Am. Chem. Soc.* **127**, 11898 (2005).
- ²⁵J. P. Camden, W. Hu, H. A. Bechtel, D. J. A. Brown, M. R. Martin, R. N. Zare, G. Lendvay, D. Troya, and G. C. Schatz, *J. Phys. Chem. A* (in press).
- ²⁶W. Hu, G. Lendvay, D. Troya, G. C. Schatz, J. P. Camden, H. A. Bechtel, D. J. A. Brown, M. R. Martin, and R. N. Zare, *J. Phys. Chem. A* (in press).
- ²⁷J. P. Camden, H. A. Bechtel, D. J. A. Brown, and R. N. Zare, *J. Chem. Phys.* **123**, 134301 (2005).
- ²⁸C. Murray and A. J. Orr-Ewing, *Int. Rev. Phys. Chem.* **23**, 435 (2004).
- ²⁹J. Zhou, J. J. Lin, B. Zhang, and K. Liu, *J. Phys. Chem. A* **108**, 7832 (2004).
- ³⁰B. Zhang and K. Liu, *J. Chem. Phys.* **122**, 101102 (2005).
- ³¹J. Zhou, B. Zhang, J. J. Lin, and K. Liu, *Mol. Phys.* **103**, 1757 (2005).
- ³²S. Yoon, R. J. Holiday, and F. F. Crim, *J. Phys. Chem. B* **109**, 8388 (2005).
- ³³B. Retail, J. K. Pearce, C. Murray, and A. J. Orr-Ewing, *J. Chem. Phys.* **122**, 101101 (2005).
- ³⁴H. A. Bechtel, J. P. Camden, D. J. A. Brown, R. M. Martin, R. N. Zare, and K. Vodopyanov, *Angew. Chem., Int. Ed.* **44**, 2382 (2005).
- ³⁵H. A. Bechtel, Z. H. Kim, J. P. Camden, and R. N. Zare, *Mol. Phys.* **103**, 1837 (2005).
- ³⁶G. Herzberg, *Infrared and Raman Spectra of Polyatomic Molecules* (Van Nostrand, New York, 1945).
- ³⁷M. S. Child and L. Halonen, *Adv. Chem. Phys.* **57**, 1 (1984).
- ³⁸M. S. Child, *Acc. Chem. Res.* **18**, 45 (1985).
- ³⁹B. R. Henry, *Acc. Chem. Res.* **10**, 207 (1977).
- ⁴⁰C. Jaffe and P. Brumer, *J. Chem. Phys.* **73**, 5646 (1980).
- ⁴¹M. S. Child and R. T. Lawton, *Faraday Discuss.* **71**, 273 (1981).
- ⁴²M. M. Law and J. L. Duncan, *Mol. Phys.* **93**, 809 (1998).
- ⁴³P. Jensen, *Mol. Phys.* **98**, 1253 (2000).
- ⁴⁴W. E. Blass and T. H. Edwards, *J. Mol. Spectrosc.* **24**, 116 (1967).
- ⁴⁵T. A. Wiggins, E. R. Shull, J. M. Bennett, and D. H. Rank, *J. Chem. Phys.* **21**, 1940 (1953).
- ⁴⁶M. Lewerenz and M. Quack, *J. Chem. Phys.* **88**, 5408 (1988).
- ⁴⁷H.-R. Dubal, T.-K. Ha, M. Lewerenz, and M. Quack, *J. Chem. Phys.* **91**, 6698 (1989).
- ⁴⁸L. Halonen and M. S. Child, *J. Chem. Phys.* **79**, 4355 (1983).
- ⁴⁹Z. H. Kim, H. A. Bechtel, and R. N. Zare, *J. Chem. Phys.* **117**, 3232 (2002).
- ⁵⁰M. W. Chase, Jr., C. A. Davies, J. R. Downey, D. J. Frurip, R. A. McDonald, and A. N. Syverud, *J. Phys. Chem. Ref. Data Suppl.* **14**, 1 (1998).
- ⁵¹R. Atkinson, D. L. Baulch, R. A. Cox, J. R. F. Hampson, J. A. Kerr, and J. Troe, *J. Phys. Chem. Ref. Data* **21**, 1125 (1992).
- ⁵²Y. Zhao, B. J. Lynch, and D. G. Truhlar, *J. Phys. Chem. A* **108**, 4786 (2004).
- ⁵³J. C. Corchado, D. G. Truhlar, and J. Espinosa-Garcia, *J. Chem. Phys.* **112**, 9375 (2000).
- ⁵⁴N. E. Shafer, A. J. Orr-Ewing, W. R. Simpson, H. Xu, and R. N. Zare, *Chem. Phys. Lett.* **212**, 155 (1993).
- ⁵⁵W. R. Simpson, A. J. Orr-Ewing, T. P. Rakitzis, S. A. Kandel, and R. N. Zare, *J. Chem. Phys.* **103**, 7299 (1995).
- ⁵⁶P. M. Regan, S. R. Langford, A. J. Orr-Ewing, and M. N. R. Ashfold, *J. Chem. Phys.* **110**, 281 (1999).
- ⁵⁷P. C. Samartzis, B. Bakker, T. P. Rakitzis, D. H. Parker, and T. N. Kitsopoulos, *J. Chem. Phys.* **110**, 5201 (1999).
- ⁵⁸J. W. Hudgens, T. G. DiGiuseppe, and M. C. Lin, *J. Chem. Phys.* **79**, 571 (1983).
- ⁵⁹J. L. Brum, R. D. Johnson III, and J. W. Hudgens, *J. Chem. Phys.* **98**, 3732 (1993).
- ⁶⁰J. Zhou, J. J. Lin, W. Shiu, S. C. Pu, and K. Liu, *J. Chem. Phys.* **119**, 2538 (2003).
- ⁶¹A. M. Mebel and S.-H. Lin, *Chem. Phys.* **215**, 329 (1997).